SUPPLEMENTAL INFORMATION

Figure S1

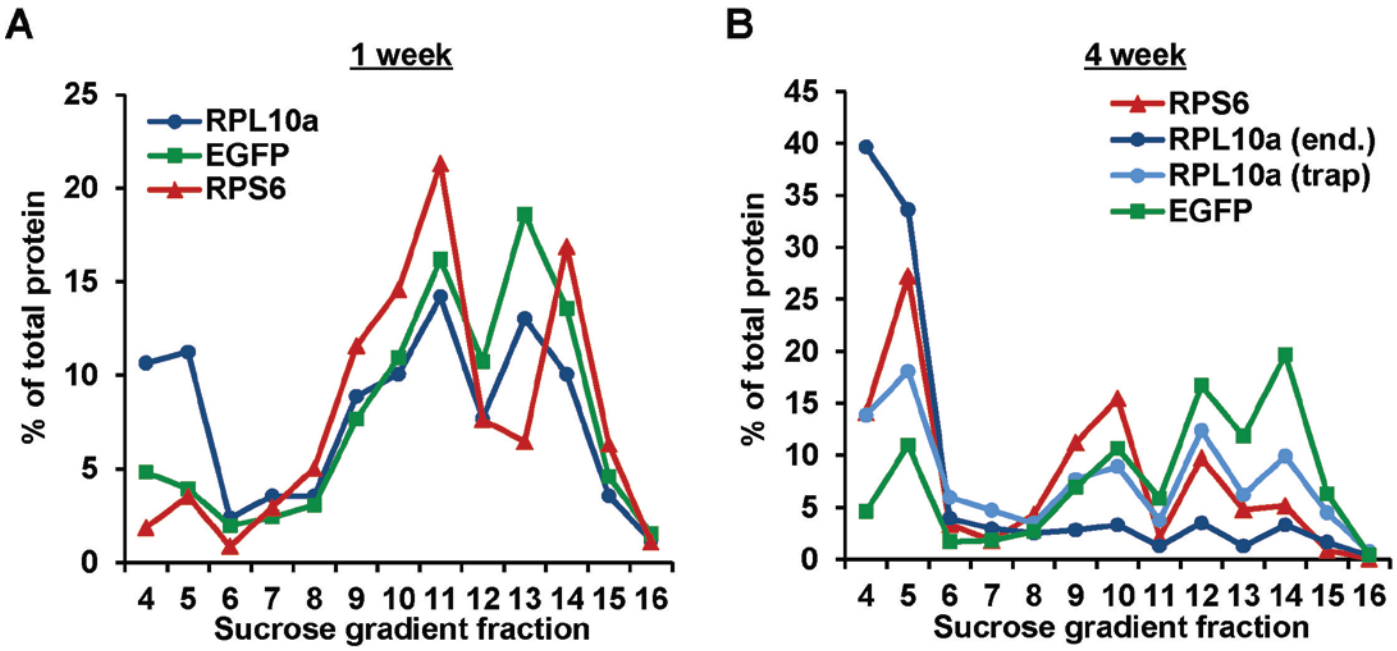

Figure S1. Quantification of the Distribution of Ribosomal Proteins in Polysome Fractions, Related to Figure 1.
(A) The distribution of RPS6, endogenous RPL10a, and EGFPL10a was quantified for each sucrose gradient fraction after one week of AAV-FLEX-EGFPL10a virus expression in Emx1-Cre cortex. The optical densities (OD) of each band on the Western blots from Figure 1E are shown as a percent of the sum of ODs across all fractions for each protein. The relative distribution of all three proteins overlapped across fractions.
(B) Quantification of the distribution of ribosomal proteins after four weeks of expression was calculated as in A. The distribution of both endogenous RPL10a (end.) and EGFPL10a (trap) were quantified from the anti-RPL10a blot. While the relative pattern of distribution of each protein was consistent across each fraction, a significant amount of endogenous RPL10a was found in fractions 4 and 5 (corresponding to the 60S subunit and monosomes, respectively), leading to comparatively lower amounts of endogenous RPL10a in polysome fractions.

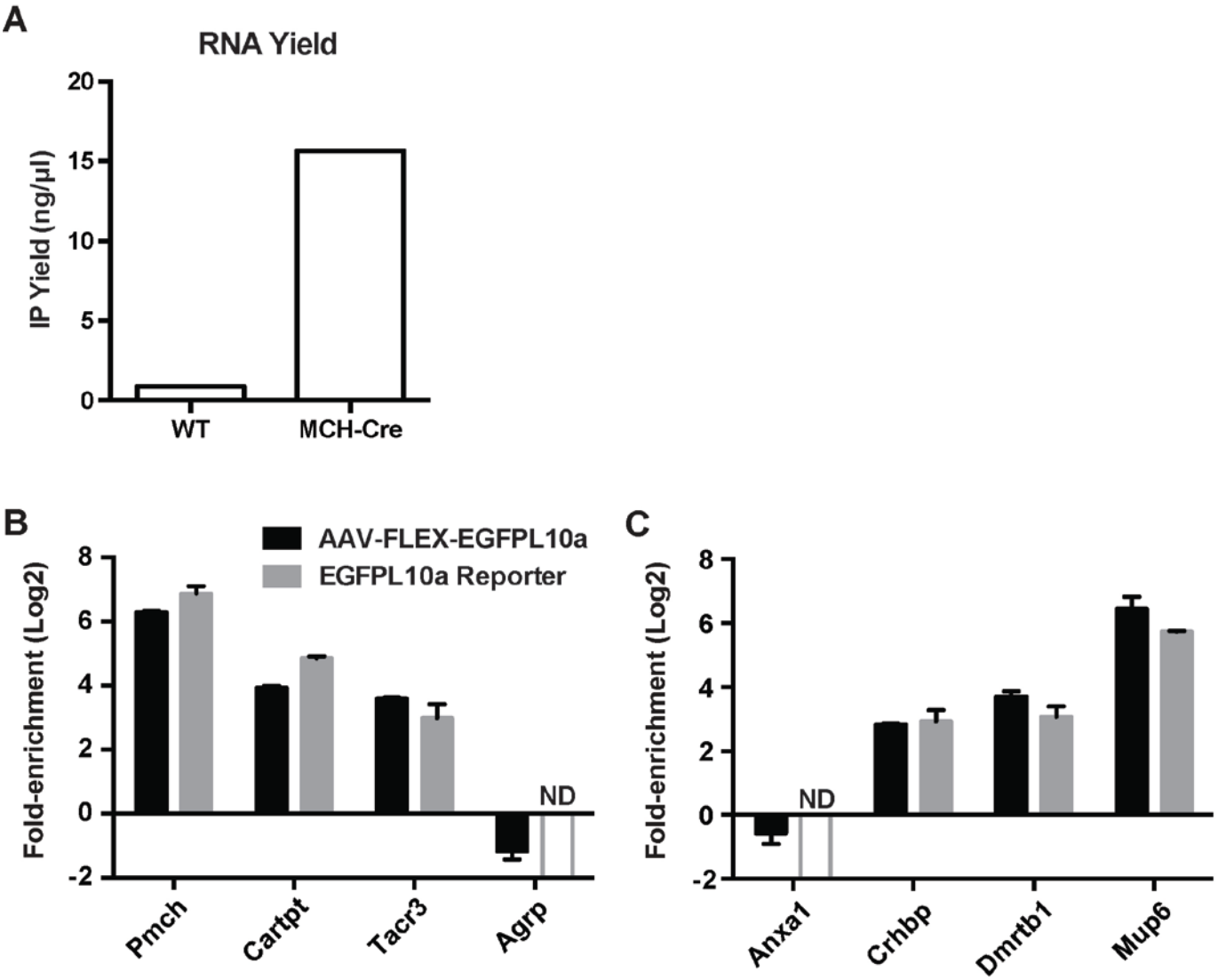

Figure S2. Comparative Enrichments from MCH Neurons using vTRAP and an EGFPL10a Reporter Mouse, Related to Figure 3.

(A) Total RNA yields after TRAP IPs in Pmch-Cre (MCH-Cre) mice or wildtype littermates (WT) following AAV-FLEX-EGFPL10a injections into the lateral hypothalamus.

(B) Quantitative RT-PCR comparison of MCH neuron marker genes (*Pmch*, *Cartpt*, *Tacr3*) and a non-MCH, hypothalamic (arcuate) marker gene (*Agrp*) after IPs from the hypothalamus of Pmch-Cre mice using vTRAP (black bars) or crossed to the Rosa26^{fsTRAP} reporter (gray bars).

(C) Quantitative RT-PCR comparison of a non-MCH neuron, midbrain marker gene (*Anxa1*), and newly-identified MCH neuron marker genes (*Crhbp*, *Dmrtb1*, *Mup6*) after IPs from the hypothalamus using vTRAP (black bars) or Rosa26^{fsTRAP} reporter (gray bars).

All data are displayed as mean ± SEM. ND, the IP RNA was not detected.

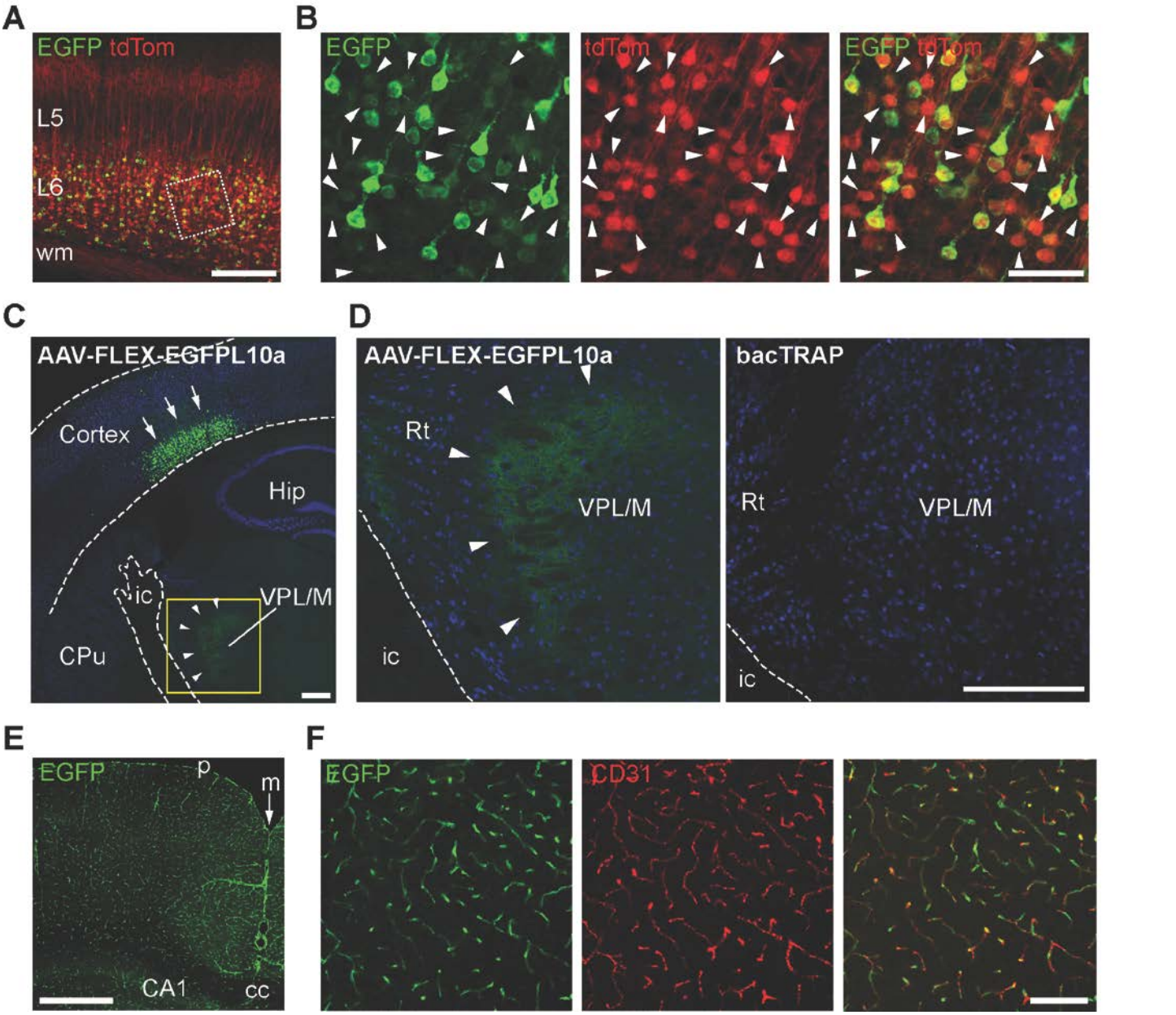

Figure S3. Co-labeling of L6 Cells by Ntsr1-bacTRAP and Ntsr1-Cre, and EGFPL10a Expression in Abcb1a-bacTRAP Mice, Related to Figures 4 and 5.

(A) Low magnification image of EGFP (green) and tdTomato (tdTom; red) immunofluorescence in cortex from a Ntsr1-bacTRAP::Ntsr1-Cre::Rosa26^{tdTomato} mouse showing all labeled cells restricted to layer 6. L5, cortical layer 5; L6, cortical layer 6; wm, white matter. Scale bar, 200 µm.

(B) Higher magnification of boxed area in A showing co-labeling of EGFP and tdTomato in L6 cells. The expression levels of EGFP varied throughout the population, likely due to the activity of the BAC promoter, nearly all tdTomato+ cells were EGFP+ and vice versa. Arrowheads indicate double-labeled cells with very low EGFP expression. Scale bar, 50 µm.

(C) Low magnification image of EGFP (green) and NeuN (blue) immunofluorescence from a brain of a Ntsr1-Cre mouse that received an injection of AAV-FLEX-EGFPL10a into somatosensory cortex. EGFP expression can be seen in the cell bodies in the cortex (arrows) as well as the axon terminal fields in the thalamus (arrowheads). CPu, caudate-putamen; Hip, hippocampus; ic, internal capsule; VPL/M, ventral posterolateral and ventral posteromedial nuclei of thalamus. Scale bar, 250 µm.

(D) Left panel shows a higher magnification of the boxed area in C and the right panel is the equivalent region from a Ntsr1-bacTRAP mouse. Note the visible EGFP expression in the axon terminal fields of a Cre mouse injected with the AAV-FLEX-EGFPL10a virus (arrowheads) but not in the bacTRAP mouse. ic, internal capsule; Rt, reticular thalamic nucleus; VPL/M, ventral posterolateral and ventral posteromedial nuclei of thalamus. Scale bar, 250 µm.

(E) Low magnification image of anti-EGFP immunofluorescence in cortex from an Abcb1a-bacTRAP ES3026 mouse. CA1, CA1 field of hippocampal formation; cc, corpus collosum; m, midline; p, pial surface. Scale bar, 500 µm.

(F) Higher magnification image of cortex of Abcb1a-bacTRAP mouse showing co-labeling of anti-EGFP (green) with andti-CD31, an endothelial cell marker (Pecam1, red). Scale bar, 100 µm.

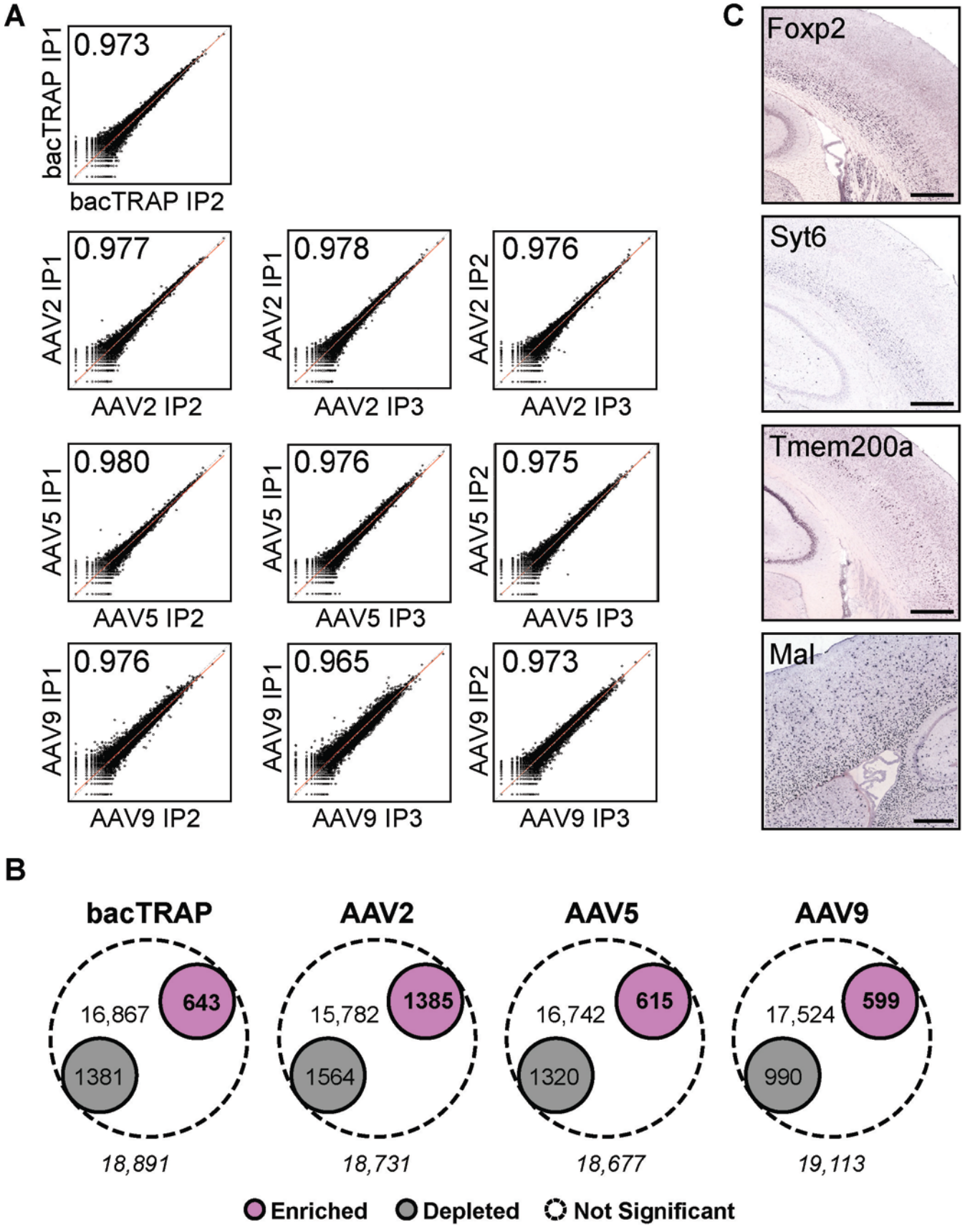

Figure S4. Correlation of bacTRAP and vTRAP Replicates and Quantification of Differentially Expressed Genes Between IP

and Input Samples, Related to Figure 4.

(A) Scatter plots comparing the normalized counts of all genes between individual replicate IPs from bacTRAP and vTRAP samples from AAV2, AAV5, and AAV9. The coefficient of determination (r^2) for each comparison is displayed in the top left corner.

(B) Venn diagrams indicating the number of genes significantly enriched in the TRAP IP (purple), the number of genes significantly depleted from the IPs (gray) and the number of genes not enriched or depleted in the bacTRAP and vTRAP experiments. Total number of genes with mapped reads in each experiment is in italics at the bottom.

(C) ABA ISH showing the cortex expression of neuronal genes *Foxp2* (layer 6, coronal), *Syt6* (layer 6, coronal), *Tmem200a* (layer 5, coronal), and the oligodendroglia marker, *Mal* (sagittal). Scale bars, 500 μm.

Figure S5

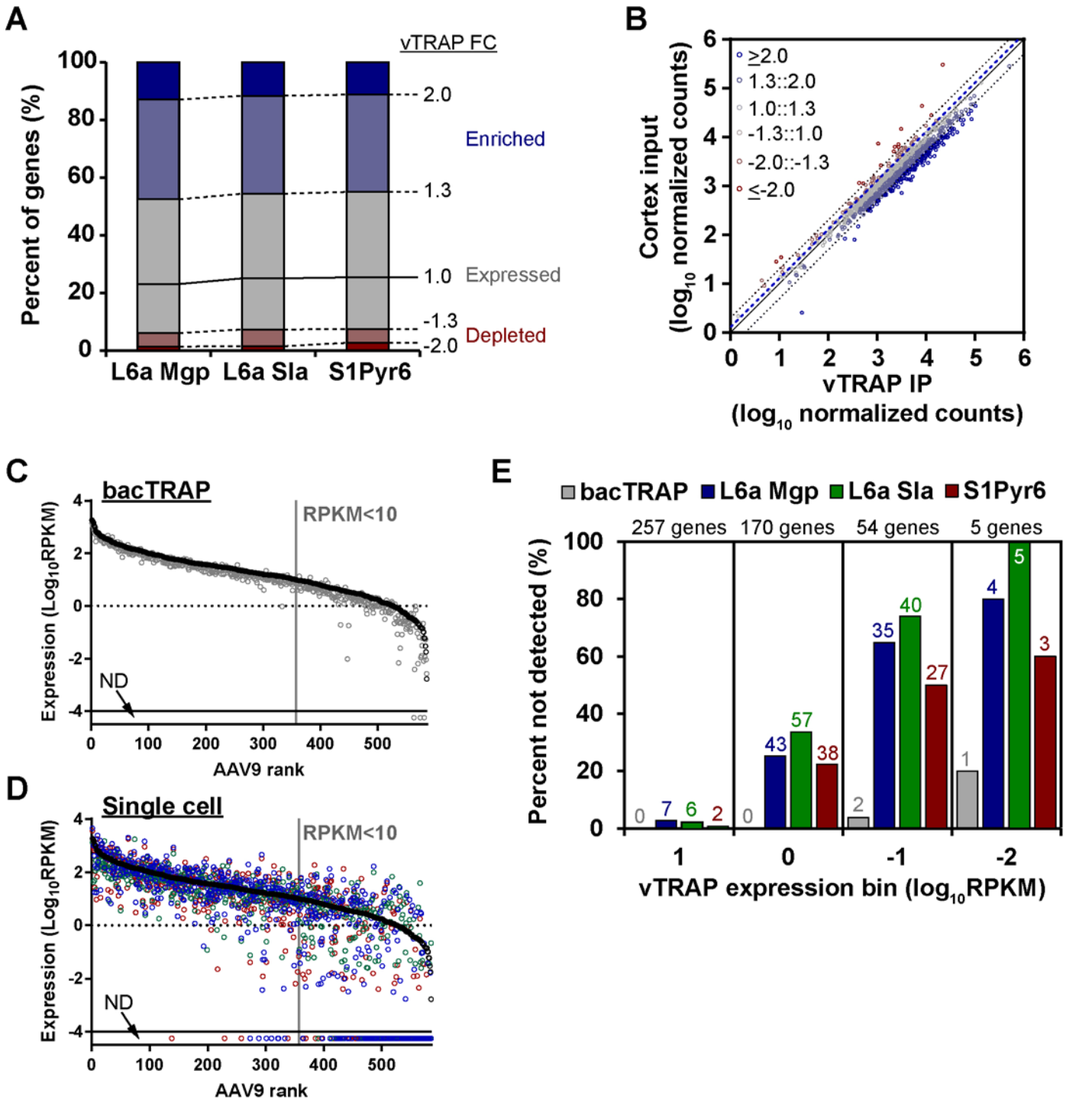

Figure S5. Comparison of vTRAP to Representative Single Cell RNA-seq Data Sets, Related to Figure 5.

(A) The top 1000 highest expressed genes were identified for three published single cell RNA-seq data sets comprised of layer 6 pyramidal cell populations: "L6a Mgp," "L6a Sla," (Tasic 2016) and "S1Pyr6" (Zeisel 2015). For each gene, the fold change was determined in the AAV9 vTRAP IP over input and the proportion of genes highly enriched (dark blue), enriched (light blue), expressed (not strongly enriched or depleted, gray), depleted (light red), or highly depleted (dark red) were plotted in a stacked bar graph. The fold change cutoff for each category is indicated on the right (vTRAP FC). More than 75% of the genes on each data set had a fold change >1.0 (over 92% of the genes from each data set were in the "expressed" range or higher) with over 45% being enriched greater than 1.3-fold in the IPs, demonstrating the sensitivity of vTRAP.

(B) Scatter plot of vTRAP IP (x-axis) and whole cortex input (y-axis) normalized counts for the top 1000 genes expressed in the L6a Mgp single cell data set. Genes are colored based on vTRAP fold change bins as in A. Dotted lines show 2-fold enrichment and depletion and solid gray line indicates the origin. Dashed blue line shows -1.3-fold change, with "expressed" genes found to the right of the line.

(C) vTRAP enriched genes (log_2FC>1) were ranked based on their expression (log_{10}RPKM) from highest to lowest (left to right) expression values were plotted for vTRAP IPs (black circles) and bacTRAP IPs (gray circles). The bar at the bottom indicates genes where RPKM=0 (not detected, ND). The bacTRAP expression values correlate very highly with those of vTRAP, with only three low-expressed genes failing to be detected by bacTRAP.
(D) vTRAP enriched genes are plotted as in C with the expression values from three single cell data sets (L6a Mgp, blue; L6a Sla, green; S1Pyr6, red). The comparative expression for each gene was much more variable compared to bacTRAP (C), and many low-expressed genes in the vTRAP data were not detected in the single cell samples.
(E) Low expressed vTRAP genes were binned based on expression and the percent of genes in each bin with RPKM=0 in bacTRAP and single cell data sets was quantified. The total number of genes in each bin is indicated at the top and the number of genes not detected is written above each bar.

Figure S6

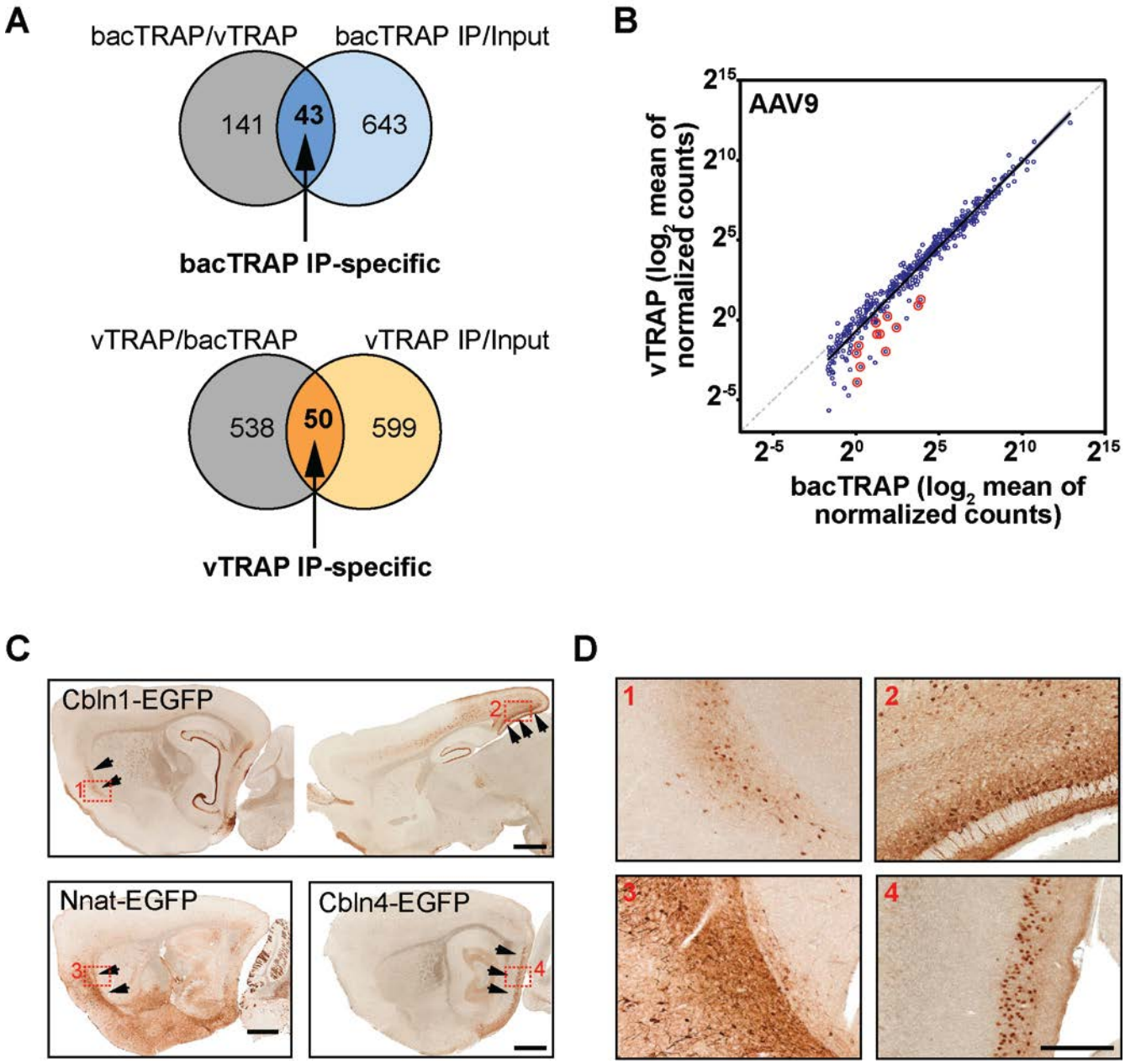

Figure S6. Identification of VTRAP-Specific and bacTRAP-Specific Genes, Related to Figure 6.

(A) Venn diagrams illustrating the definition of bacTRAP IP-specific genes as the union (blue) of genes significantly enriched in bacTRAP IP versus whole cortex input and bacTRAP IP versus vTRAP IP (top), and the definition of vTRAP IP-specific genes as the union (orange) of genes significantly enriched in vTRAP IP versus whole cortex input and vTRAP IP versus bacTRAP IP (bottom). vTRAP samples were from AAV9 injections. All significant genes had $\log_2$ fold change >1.0 and FDR <0.1.

(B) Genes with regional expression (red circles) are indicated on the scatter plot from Figure 5C comparing the expression of CThal specific genes (pSI<0.05; blue circles) between Ntsr1 bacTRAP (x-axis) and AAV9 vTRAP (y-axis). Regional genes account for a majority of the CThal specific genes that are considerably enriched in the bacTRAP samples.

(C) Anti-EGFP immunolabeling of BAC reporter lines showing expression patterns of some regionally expressed genes absent from vTRAP data set. Arrowheads identify regions with high expression in cells. Scale bars, 1 µm.

(D) High magnification images from boxed areas in D. Scale bar, 200 µm. Images in D and E are from The Gene Expression Nervous System Atlas (Gong et al., 2003) (www.gensat.org). Scale bars, 200 µm.

Table S1. bacTRAP Transgenic Mouse Strains used for Specificity Index, Related to Figure 5.

Driver Gene	Founder	Cell type	Reference
Abcb1a	ES3026	Blood vessels	This paper
Aldh1l1	JD130	Astrocytes	Doyle et al. (2008)
Dlx1	GM520	Fast-spiking interneurons	Nakajima et al. (2014)
Glt25d2	DU9	Layer 5b CPn neurons	Doyle et al. (2008)
Ntsr1	TS16	Layer 6 CThal neurons	Doyle et al. (2008)
S100a10	ES691	Layer 5a CStr neurons; pia	Schmidt et al. (2012)

Table S2. Ntsr1-Specific Genes (pSI<0.05), Related to Figure 5.

The Specificity Index algorithm (Dougherty et al., 2010) was used to generate a list of genes specific for Ntsr1-expressing neurons compared to other cell types in the cortex (see Supplementary Table 1). The rank of each gene in each cell type and pSI is indicated. (Table is attached at the end of this document.)

Table S3. Previously identified cell type specific genes, Related to Figure 5.

This table contains a compiled list of genes that were previously shown to label L6 projection neurons or glial cells by a variety of distinct methodologies. The log2 fold change (TRAP IP/input) of each gene is shown for each replicate of bacTRAP and vTRAP data sets. In addition, a summary of the methodology used, the cell type ID, and a hyperlink to the original source are also included. Genes appearing multiple times on the list are shown in bold. For glial genes, only the top 10 genes from each study are listed for each cell type. (Table is attached at the end of this document.)

Table S4. Images of Gene Expression Obtained from Public Databases, Related to Figures 6 and S3.

I. Allen Mouse Brain Atlas (mouse.brain-map.org)

Figure	Symbol	Gene Name	Plane	Experiment	Image
6C	*Cbln1*	cerebellin 1 precursor protein	sagittal	100145395	61
6C	*Cbln1*	cerebellin 1 precursor protein	sagittal	100145395	109
6C	*Col23a1*	collagen, type XXIII, alpha 1	sagittal	71579924	110
6C	*Ly6g6e*	lymphocyte antigen 6 complex, locus G6E	sagittal	75198208	112
6C	*Nnat*	neuronatin	sagittal	77790710	41
6C	*Nnat*	neuronatin	sagittal	77790710	113
6D	*Ntsr1*	neurotensin receptor 1	sagittal	80342232	29
6E	*Cbln4*	cerebellin 4 precursor protein	sagittal	69540435	26
6E	*Cldn1*	claudin 1	sagittal	75695650	33
6E	*Fam70b*	family with sequence similarity 70, member B	sagittal	70298238	14
6E	*Lef1*	lymphoid enhancer binding factor 1	sagittal	77464846	28
6E	*Mum1l1*	melanoma associated antigen (mutated) 1-like 1	sagittal	71494629	42
6E	*Pth2r*	parathyroid hormone 2 receptor	sagittal	69863250	40
S3D	*Foxp2*	forkhead box P2	coronal	72079884	264
S3D	*Mal*	myelin and lymphocyte protein, T cell differentiation protein	sagittal	386243	101
S3D	*Syt6*	synaptotagmin VI	coronal	1032	215
S3D	*Tmem200a*	transmembrane protein 200A	coronal	79591403	262

II. GENSAT (www.gensat.org)

Figure	Symbol	Gene Name	Plane	Founder	Age	Section
S5D	*Cbln1*	cerebellin 1 precursor protein	sagittal	JD6	Adult	02
S5D	*Cbln1*	cerebellin 1 precursor protein	sagittal	JD6	Adult	08
S5D	*Nnat*	neuronatin	sagittal	EA106	Adult	03
S5D	*Cbln4*	cerebellin 4 precursor protein	sagittal	IG145	Adult	02

SUPPLEMENTAL EXPERIMENTAL PROCEDURES

Animals

All procedures involving animals were approved by The Rockefeller University Institutional Animal Care and Use Committee and were in accordance with National Institutes of Health guidelines. Ntsr1-bacTRAP (TS16), Pmch-Cre, and DAT-Cre mice were generated and maintained at The Rockefeller University and described previously (Doyle et al., 2008; Ekstrand et al., 2014; Jego et al., 2013; Knight et al., 2012). Ntsr1-Cre (GN220) and SERT-Cre (ET33) mice were generated by the GENSAT Project (Gong et al., 2007) and were purchased from the Mutant Mouse Regional Resource Center (Stock IDs 017266-UCD and 031028-UCD, respectively). Rosa26^{tdTomato} (Stock #007914) and Rosa26^{fsTRAP} (Stock #022367) mice were purchased from The Jackson Laboratories. All mice were bred on a C57BL/6J background and maintained on a 12 hr light-dark cycle. Animals used in the study were male and female. Mice were sacrificed at 10-20 weeks of age within the same circadian period (12:00-16:00).

To generate the Abcb1a-bacTRAP mice, the RP24-384G12 BAC, which contained the Abcb1a locus, was modified using the two-plasmid/one recombination protocol as described previously (Gong et al., 2010; Gong et al., 2002). Briefly, a homology arm corresponding to the region immediately upstream of the ATG translation initiation site of the *Abcb1a* gene was cloned into the pS296 targeting vector (Heiman et al., 2008) containing EGFPL10a using the *AscI* and *NotI* restriction sites. Recombination was performed by electroporating the pS296-Abcb1a vector into electrocompetent DH10β bacteria containing pSV1.RecA plasmid and the BAC. Successful recombination was determined by screening cointegrates by PCR and Southern blot analysis of *HindIII* digested BAC DNA, using the homology region as a probe. The modified BAC was prepared by double acetate purification with CsCl centrifugation followed by membrane dialysis and microinjected into the pronuclei of fertilized FVB/N mouse oocytes at a concentration of 0.5 ng/µl. Six transgenic founder mice were generated and crossed to C57BL/6J mice. F1 progeny were screened for proper transgene expression by EGFP immunohistochemistry. Founder line ES3026 showed accurate and robust expression of the transgene and was therefore selected for colony expansion.

Generation of AAVs

The plasmid pAAV-FLEX-EGFPL10a was generated in an analogous fashion to pAAV-FLEX-NBL10 (Ekstrand et al., 2014). Briefly, the EGFPL10a transgene was PCR amplified from the pS296 targeting vector (Heiman et al., 2008) adding 5' NheI and 3' AscI restriction sites. The amplicon was then subcloned into pAAV-EF1a-DIO-hChR2 (H134R)-mCherry-WPRE-HGHpA (Addgene plasmid #20297) in the reverse orientation using NheI and AscI sites, replacing ChR2-mCherry, to create pAAV-FLEX-EGFPL10a. Plasmids were then packaged into AAVs serotyped with AAV5 capsids at the University of North Carolina Vector Core or AAV2 and AAV9 capsids at the University of Pennsylvania Vector Core. Virus titers were $1.63x10^{13}$ gc/ml for AAV5, $4.7x10^{12}$ gc/ml for AAV2, and $7.47x10^{12}$ gc/ml for AAV9.

Stereotaxic Surgeries

Surgeries were performed on adult mice (8-20 weeks old) under ketamine/xylazine (100/10 mg/kg) anesthesia. Single bilateral stereotaxic injections of 0.25-1.0 µl pAAV-FLEX-EGFPL10a were done using the following injection sites: DRN, +0.8 mm ML, 0 mm AP from lambda, -3.0 mm DV from dura, injected at a 15° angle; VTA ± 1.0 ML, -3.15 AP from bregma, -4.23 DV from dura, injected at a 7°angle; LH ±1.56 ML, -1.2 AP from bregma, -4.75 DV, injected at a 8° angle; S1BF, ±2.5 ML, -1.0 AP from bregma, -0.75 DV from dura. For S1BF injections, a single bilateral injection of 0.25 µl virus into S1BF was done for each serotype. Following injections, the needle was slowly retracted and skin was closed with a surgical clip. Animals were sacrificed 3-4 weeks after surgery and tissue was collected for polysome immmunoprecipitations or immunohistology as described. For polysome fractionation experiments, 0.3 µl AAV9 pseudotyped pAAV-FLEX-EGFPL10a virus was bilaterally injected into S1BF at three sites spaced 0.2 mm apart in the AP plane of Emx1-Cre mice. Mice were sacrificed for polysome biochemistry either one week or four weeks after surgery (see below).

Immunohistochemistry

Mice were deeply anesthetized and transcardially perfused with PBS followed by 4% paraformaldehyde in PBS. Brains were dissected and postfixed for 8-12 hours at 4°C, cryopreserved in 30% sucrose solution, and sectioned on a freezing microtome (35 µm sections). Free-floating sections were immunofluorescently stained with chicken anti-GFP (1:2000, Abcam, Cambridge, MA, Cat# ab13970), mouse anti-NeuN (1:1000, Millipore, Billerica, MA, Cat# MAB377B), anti-TH (1:1000, Pel-Freez, Rogers, AR), anti-TPH2 (1:500, Novus Biologicals, Littleton, CO, Cat# NB100-74555), and anti-MCH (1:1000, Phoenix Pharmaceuticals, Berlingame, CA) primary antibodies. Sections were blocked for 60 min in PBS containing 2.5% normal goat serum (NGS) and 0.1% Triton-X-100 and then incubated overnight at 4°C with primary antibodies diluted in PBS containing 11% NGS and 0.1% Triton-X-100. Sections were washed with PBS and incubated for one hour at room temperature with Alexa-fluor conjugated secondary antibodies (Life Technologies, Waltham, MA) diluted in PBS. All sections were imaged on either a Zeiss LSM780 or LSM700 confocal microscope.

For cell culture experiments, HEK293T cells were co-transfected with pAAV-FLEX-EGFPL10a and pCAG-Cre (Addgene plasmid #13775) using the Fugene-6 transfection method (Roche Diagnostics, Indianapolis, IN). After 36 hours, cells were fixed with 4% paraformaldehyde in PBS and visualized by immunofluorescent staining with chicken anti-GFP (as above) and mouse anti-c-Myc clone 9E10 (1:1000, Sigma-Aldrich, St. Louis, MO, Cat# M5546) primary antibodies followed by Alexa Fluor-488-conjugated goat anti-chicken and Alexa Fluor-568-conjugated goat anti-mouse secondary antibodies. Cells were then coverslipped and imaged on a Zeiss LSM700 confocal microscope.

Translating ribosome affinity purification

Affinity purification of EGFP-tagged polysomes was carried out as previously described (Heiman et al., 2014). IPs were done 3-4 weeks after viral injections and three biological replicates consisting of brain tissue pooled from 3-5 mice (male and female) were

used for each condition. Mice were sacrificed, followed by rapid dissection of brain tissue in ice-cold HBSS containing 2.5 mM HEPES-KOH (pH 7.4), 35 mM glucose, 4 mM $NaHCO_3$, and 100 µg/ml cycloheximide. Tissue containing relevant brain regions (e.g. whole cortex, hypothalamus) was then homogenized in extraction buffer containing 10 mM HEPES-KOH (pH 7.4), 150 mM KCl, 5 mM $MgCl_2$, 0.5 mM DTT, 100 µg/ml cycloheximide, RNasin (Promega, Madison, WI) and SUPERas-In^{TM} (Life Technologies) RNase inhibitors, and Complete-EDTA-free protease inhibitors (Roche), and then cleared by centrifugation at 2000 x g. IGEPAL CA-630 (NP-40, Sigma) and DHPC (Avanti Polar Lipids, Alabaster, AL) were both added to the S2 supernatant to a final concentration of 1% for each, followed by centrifugation at 20,000 x g. Polysomes were immunoprecipitated from the S20 supernatant using 100 µg monoclonal anti-EGFP antibodies (50 µg each of clones 19C8 and 19F7; see Heiman et al., 2008) bound to biotinylated-Protein L (Pierce, Thermo Fisher, Waltham, MA) coated streptavidin-conjugated magnetic beads (Life Technologies), and washed in high salt buffer containing 10 mM HEPES-KOH (pH7.4), 350 mM KCl, 5 mM $MgCl_2$, 1% IGEPAL CA-630, 0.5 mM DTT, 100 µg/ml cycloheximide, and RNasin RNase inhibitors (Promega). IPs were carried out overnight at 4°C. Bound RNA was purified using the Absolutely RNA Nanoprep kit (Agilent, Santa Clara, CA). RNA was also purified from a fraction of the pre-IP S20 supernatant to serve as whole-tissue "input" samples. RNA quantity was measured with a Nanodrop 1000 spectrophotometer and quality was assayed on an Agilent 2100 Bioanalyzer. Only samples with RNA integrity values >7.0 were used for RNA-seq and qRT-PCR analyses.

RNA-seq

For cortical samples, 15 ng of total RNA was amplified using the Ovation RNA-Seq System V2 Kit (NuGEN, San Carlos, CA) and RNA-seq libraries were prepared from 10 µg amplified RNA using the TruSeq RNA Sample Preparation Kit v2 (Illumina, San Diego, CA) following manufacturer's protocols. MCH neuron RNA-seq libraries were prepared with oligo-dT priming using the SMARTer Ultra Low RNA Kit (Clontech, Mountain View, CA). Sequencing reactions (50 b.p., single end for all Ntsr1 samples, and 100 b.p., single end for MCH samples) were done using the Illumina HiSeq 2500 platform with three samples multiplexed per sequencing lane. RNA-seq read quality was assessed with FASTX Toolkit 0.0.13 and sequences were trimmed for trailing adaptors. Trimmed reads were then aligned to annotated exons using the mm10 mouse reference genome with STAR (Dobin et al., 2013) version 2.0.0e_r291 using default settings. The numbers of raw and mapped reads for each sample are presented in the table "Quality Control of RNA-seq Alignments" below. Quantification of aligned reads was done using the htseq-count module of the HTSeq framework (Anders et al., 2015) version 0.6.0 using the "union" mode with default settings to generate raw counts for each sample. Differential expression was calculated by DESeq2 (Love et al., 2014) version 1.4.5 using default settings and filtering for an FDR cutoff of <0.05 and $|\log_2|$ fold change >1.0. For scatter plots (Figures 3D, 4B, 5C, 6A, and S5B), data are displayed as $\log_2$ mean of raw counts normalized to sample size for each sample ("normalized counts") as calculated by DESeq2. For specificity index analysis of multiple distinct cell types, cell specific gene expression quantification was carried out on DESeq2 normalized TRAP-seq counts using the pSI (Specificity Index Statistic) R-package version 1.1 (Dougherty et al., 2010). For Figures 3C and E, RNA-seq data were normalized as fragments per kilobase of transcript per million mapped reads (FPKM) using Cufflinks v2.1.1. Fold-enrichment was calculated as FPKM of GFP IP divided by FPKM Input (IP/Input). RPKMs in Figure S5C and D were calculated as: RPKM = (10^9 * Count)/(Library Size * Gene Length), with Gene Length being the maximum sum of annotated exon lengths of gene transcripts for a given gene (based on GENCODE VM9 [Ensembl 84], updated March 14, 2016). RNA-seq data sets have been deposited in NCBI's Gene Expression Omnibus (GEO; Barret et al., 2013), and are accessible through GEO Series accession number GSE89737.

For comparison of vTRAP to single cell RNA-seq results in Figure S5, raw sequence read archives (SRAs) of published single cell RNA-seq data were downloaded from NCBI's GEO. Data sets from GEO Series GSE71585 representing six individual "Core" cells from Primary Type Cells "L6a Sla" (Cell ID T02251526, GEO Sample accession GSM1839921; T01101413, GSM1839898; T02271422, GSM1839927; T01101411, GSM1839896; T07011417, GSM1839960; and T07011415, GSM1839958) and "L6a Mgp" (T07011423, GSM1839966; T05151410, GSM1839939; T05151405, GSM1839934; T02251501, GSM1839902; T01101410, GSM1839895; T02271423, GSM1839928) were randomly selected for analysis (Tasic et al., 2016). Six data sets from GEO Series GSE60361 representing "S1Pyr6" cells (Zeisel et al., 2015) were selected based on their expression of the cell-type markers *Rprm*, *Foxp2*, and *Syt6* (1772071041_E04, GSM1477180; 1772071040_F06, GSM1477141; 1772067073_G04, GSM1476683; 1772067074_C04, GSM1476697; 1772067074_G06, GSM1476721; 1772067064_A11, GSM1476528). All raw sequencing data sets were processed as described above.

Quality Control of RNA-seq Alignments.

Sample	Raw Reads	Uniquely Mapped Reads	% Uniquely Mapped Reads	% Aligned Bases Mapped to mRNA*
Ntsr1 bacTRAP IP rep 1	72,542,951	56,327,123	77.65	70.7724
Ntsr1 bacTRAP IP rep 2	69,360,209	54,582,713	78.69	74.2391
Ntsr1 AAV2 IP rep 1	67,797,151	53,303,721	78.62	74.5542
Ntsr1 AAV2 IP rep 2	57,147,662	45,017,131	78.77	75.054
Ntsr1 AAV2 IP rep 3	60,796,930	47,765,900	78.57	74.9366
Ntsr1 AAV5 IP rep 1	58,284,352	44,636,629	76.58	75.2089

Ntsr1 AAV5 IP rep 2	48,031,599	36,300,939	75.58	73.9679
Ntsr1 AAV5 IP rep 3	47,091,409	36,381,832	77.26	75.8054
Ntsr1 AAV9 IP rep 1	77,836,295	57,217,810	73.51	67.0368
Ntsr1 AAV9 IP rep 2	73,561,919	55,719,055	75.74	64.402
Ntsr1 AAV9 IP rep 3	79,455,352	62,665,474	78.87	68.0555
bacTRAP cortex input rep 1	117,570,640	96,792,310	82.33	63.4668
bacTRAP cortex input rep 2	127,417,769	101,738,934	79.85	63.5548
AAV2 cortex input rep 1	60,589,103	48,242,443	79.62	61.043
AAV2 cortex input rep 2	58,975,851	46,766,108	79.30	59.2499
AAV2 cortex input rep 3	67,119,968	52,608,978	78.38	61.3017
AAV5 cortex input rep 1	52,801,324	42,071,998	79.68	58.3502
AAV5 cortex input rep 2	56,330,442	44,226,435	78.51	54.0793
AAV5 cortex input rep 3	53,762,949	42,248,320	78.58	62.3024
AAV9 cortex input rep 1	78,811,731	62,506,741	79.31	58.4366
AAV9 cortex input rep 2	75,437,329	59,829,050	79.31	59.0644
AAV9 cortex input rep 3	77,435,616	62,244,294	80.38	61.1087
MCH IP rep 1	30,125,935	25,759,835	85.51	84.3355
MCH IP rep 2	32,654,548	27,928,690	85.53	77.4527
MCH IP rep 3	29,552,843	25,254,467	85.46	85.0989
MCH input rep 1	35,197,999	30,080,429	85.46	77.2914
MCH input rep 2	21,227,735	17,419,466	82.06	83.1531
MCH input rep 3	29,554,526	24,778,076	82.84	75.8473

*These are the percentage of total bases mapping to Coding + UTRs.

Polysome fractionation

Polysome fractionations were collected by centrifugation in a sucrose gradient as described previously(Darnell et al., 2011). Briefly, mice were sacrificed one or four weeks after AAV injection and cortices were rapidly dissected in ice-cold HBSS containing 2.5 mM HEPES-KOH (pH 7.4), 35 mM glucose, 4 mM $NaHCO_3$, and 100 µg/ml cycloheximide. Each cortex (two hemispheres) was homogenized in 1 ml gradient buffer containing 20 mM HEPES-KOH (pH 7.4), 150 mM NaCl, 5 mM $MgCl_2$, 0.5 mM DTT, 100 µg/ml cycloheximide, RNasin RNase inhibitors (Promega), and Complete-EDTA-free protease inhibitors (Roche), and then cleared by centrifugation at 2000 x g at 4°C. IGEPAL CA-630 (NP-40, Sigma) was added to the S2 supernatant to a final concentration of 1% followed by centrifugation at 20,000 x g at 4°C. The S20 supernatant was then loaded onto a 20%–50% w/w linear density gradients of sucrose in 10mM HEPES–KOH, pH 7.4, 150mM NaCl, 5mM MgCl2 and centrifuged at 40,000 r.p.m. for 2 hr at 4°C in a Beckman Instruments (Fullerton, CA) SW41 rotor. Fractions of 0.69 ml volume were collected with continuous monitoring at 254 nm using an ISCO UA-6 UV detector (ISCO, Inc, Lincoln, NE). TCA-precipitated proteins from 200 µl of each fraction were analyzed by Western blot, separated on 8% tris-glycine polyacrylamide gels (Novex, Thermo Fisher) and transferred to Optitran BA-S83 membranes (Whatman, Sigma-Aldrich) by standard methods. Membranes were blocked for 1hr at room temperature in 5% non-fat dry milk (Carnation) in PBS followed by addition of primary antibody for 1 hr at room temperature or overnight at 4 degrees. Blots were washed 4 X 5 min with Western blot wash buffer (23mM Tris, pH 8.0, 190mM NaCl, 0.1% w/v BSA, 1 mM EDTA, 0.5% Triton X-100, 0.02% SDS) after each antibody incubation. HRP-conjugated secondary antibodies (Jackson Immuno Research, West Grove, PA) were used at 1:10,000 in 5% milk/PBS for 1 hr at RT, blots were washed as before, and HRP signal was detected by enhanced chemiluminescence (Western Lightning Plus detection kit, Perkin Elmer, Waltham, MA) followed by quantification by densitometry of scanned films (Kodak MR film, ImageJ software). Primary antibodies were anti-RPL10a mouse monoclonal antibody (M01), clone 3G2 (Abnova Corporation, Walnut, CA, Cat# H00004736-M01) at 1:1,000; anti-GFP mouse monoclonal (B-2; Santa Cruz Biotechnology, Dallas, TX, Cat# sc-9996) at 1:200; and anti-RPS6 rabbit monoclonal antibody (5G10; Cell Signaling Technology, Danvers, MA,Cat# 2217).

Quantitative RT-PCR

qRT-PCR was performed on either an Applied Biosystems 7500 Fast or StepOnePlus Fast Real-Time PCR System using Taqman assays (see table below titled "TaqMan Gene Expression Assays used for qPCR") and following standard cycling conditions (50°C for 2 min, 95°C for 10 min, then 40 cycles of 95°C for 15 s and 60°C for 1 min). Ten nanograms of cDNA prepared independently from the RNA-seq libraries were used for each qRT-PCR reaction and technical triplicates were run for three biological replicates for each condition. The mean C_T for technical replicates was used for quantification. For Figures 2C, 3B and S2, data are normalized to *Rpl23* expression by standard curve. For Figures 4D and 6G, data are normalized to *Actb* by the comparative C_T ($2^{-\Delta\Delta CT}$) method (Livak and Schmittgen, 2001). Data are presented as mean ± SEM of biological triplicates.

TaqMan Gene Expression Assays used for qPCR.

Symbol	Gene Name	Source	Assay	Dye
Actb	actin, beta	Life Technol.	Mm00607939_s1	FAM
Agrp	agouti-related peptide	IDT DNA	Mm.PT.56a.31030782.gs	FAM
Anxa1	annexin A1	IDT DNA	Mm.PT.58.12626377	FAM
Cartpt	cocaine- and amphetamine-regulated transcript	IDT DNA	N001081493.1.pt.Cartpt	FAM
Cbln1	cerebellin 1 precursor protein	Life Technol.	Mm01247194_g1	FAM
Cbln4	cerebellin 4 precursor protein	Life Technol.	Mm01249788_m1	FAM
Cldn1	claudin 1	Life Technol.	Mm00516701_m1	FAM
Crhbp	corticotropin releasing hormone binding protein	IDT DNA	Mm.PT.56a.8159672	FAM
Dmrtb1	dmrt-like family B with proline-rich c-terminal, 1	IDT DNA	Mm.PT.58.43084043	FAM
Fev	fev (ets oncogene family)	IDT DNA	Mm.PT.56a.8125305	FAM
Foxp2	forkhead box P2	Life Technol.	Mm00475030_m1	FAM
Mal	myelin and lymphocyte protein, T cell differentiation protein	Life Technol.	Mm01339780_m1	FAM
Mup6	major urinary protein 6	IDT DNA	Mm.PT.58.42371435	FAM
Nnat	neuronatin	Life Technol.	Mm00731416_s1	FAM
Ntsr1	neurotensin receptor 1	Life Technol.	Mm00444459_m1	FAM
Pmch	pro-melanin concentrating hormone	IDT DNA	N029971.1.pt.Pmch	FAM
Pth2r	parathyroid hormone 2 receptor	Life Technol.	Mm00653029_m1	FAM
Rpl23	ribosomal protein L23	IDT DNA	Mm.PT.56a.10484606.g	FAM
Slc6a3	dopamine transporter		Homemade assay	FAM
Slc6a4	serotonin transporter	IDT DNA	Mm.PT.56a.43910045	FAM
Slc32a1	vesicular GABA transporter	IDT DNA	Mm.PT.58.6658400	FAM
Syt6	synaptotagmin VI	Life Technol.	Mm01308768_m1	FAM
Tacr3	tachykinin 3 receptor	IDT DNA	Mm.PT.42.6434400	FAM
Th	tyrosine hydroxylase		Homemade assay	FAM
Tmem200a	transmembrane protein 200A	Life Technol.	Mm01190399_m1	FAM

Scoring Allen Mouse Brain Atlas in situ hybridizations

The expression pattern of "bacTRAP-specific" and "vTRAP-specific" genes was qualitatively scored by a blinded observer using the Allen Mouse Brain Atlas ISH database for adult mouse brain(Lein et al., 2007). All scores were done using sagittal data sets since this orientation is available for all genes in the database. When available, coronal data sets were used to confirm the score since this orientation provides the most direct assessment of laminar and areal subdivisions of cortex. A gene was scored as "Regional" if there had distinct ISH signal (at least two color levels above values of neighboring areas of cortex in the ABA "expression viewer") in layer 6 of the neocortex in rostral and/or caudal regions that did not overlap with the AAV injection site (green ovals in Figure 6C), or expression was restricted to the AAV injection site and not found at rostral or caudal regions. Genes widely absent from the neocortex but with distinct ISH signal in entorhinal cortex were also scored as "Regional" due to entorhinal cortex labeling in the Ntsr1-bacTRAP (TS16) mouse line. Additionally, genes were scored as "Widespread" if expression was distributed throughout the rostral-caudal plane of layer 6 of the neocortex, or seen in in layer 6 as well as other layers, "No Signal" if the ISH had no detectable signal anywhere in the brain or was of low quality (no signal above the lowest color level in the "expression viewer"), "Not Expressed" if there was no expression within layer 6 of neocortex (but clear expression elsewhere), or "No Data" if the gene was not found in the data base.

Statistics

All data analysis was performed in Graphpad Prism, Microsoft Excel, or R (R Core Team, 2013). Student's t-test was used to compare differences in qRT-PCR results between IP and input samples in Figures 2D, 3F, 4D, and 6G. Two-way ANOVA on the $\log_2$ fold change values was used to compare each of the vTRAP groups against bacTRAP for the specified genes in Figures 4D and 6G. Statistical methods used to analyze RNA-seq data are discussed in the "RNA-seq" section.

SUPPLEMENTAL REFERENCES

Barrett T, Wilhite SE, Ledoux P, Evangelista C, Kim IF, Tomashevsky M, Marshall KA, Phillippy KH, Sherman PM, Holko M, Yefanov A, Lee H, Zhang N, Robertson CL, Serova N, Davis S, Soboleva A. (2013). NCBI GEO: archive for functional genomics data sets--update. Nucleic Acids Res *41*, D991-5. 10.1093/nar/gks1193

Gong, S., Kus, L., and Heintz, N. (2010). Rapid bacterial artificial chromosome modification for large-scale mouse transgenesis. Nat Protoc *5*, 1678-1696. 10.1038/nprot.2010.131

Gong, S., Zheng, C., Doughty, M.L., Losos, K., Didkovsky, N., Schambra, U.B., Nowak, N.J., Joyner, A., Leblanc, G., Hatten, M.E., *et al.* (2003). A gene expression atlas of the central nervous system based on bacterial artificial chromosomes. Nature *425*, 917-925.

Gong, S., Yang, X.W., Li, C., and Heintz, N. (2002). Highly efficient modification of bacterial artificial chromosomes (BACs) using novel shuttle vectors containing the R6Kgamma origin of replication. Genome Res *12*, 1992-1998.